Discrete conformations of epitope II on the hepatitis C virus E2 protein for antibody-mediated neutralization and nonneutralization

Lu Deng[a], Li Ma[a], Maria Luisa Virata[a], Lilin Zhong[a], Hailing Yan[a], Zhong Zhao[a], Evi Struble[a], Stephen Feinstone[b], Harvey Alter[c,1], and Pei Zhang[a,1]

[a]Division of Hematology, Office of Blood Research and Review, Center for Biologics Evaluation and Research, US Food and Drug Administration, Bethesda, MD 20892; [b]Department of Biochemistry and Molecular Medicine, George Washington University School of Medicine and Health Sciences, Washington, DC 20037; and [c]Department of Transfusion Medicine, Warren Grant Magnuson Clinical Center, National Institutes of Health, Bethesda, MD 20892

Contributed by Harvey Alter, June 17, 2014 (sent for review April 4, 2014)

The X-ray crystal structure of epitope II on the E2 protein of hepatitis C virus, in complex with nonneutralizing antibody mAb#12, has been solved at 2.90-Å resolution. The spatial arrangement of the essential components of epitope II (ie, the C-terminal α-helix and the N-terminal loop) was found to deviate significantly from that observed in those corresponding complexes with neutralizing antibodies. The distinct conformations are mediated largely by the flexibility of a highly conserved glycine residue that connects these components. Thus, it is the particular tertiary structure of epitope II, which is presented in a spatial and temporal manner, that determines the specificity of antibody recognition and, consequently, the outcome of neutralization or nonneutralization.

immunoglobulins | prophylaxis | vaccine

Hepatitis C is a major public health problem worldwide. More than 170 million people are infected by the hepatitis C virus (HCV) (1). Approximately 70% of infected people fail to clear the virus during the acute phase of the disease and become chronic carriers (2). Liver cirrhosis, which develops in about 10–20% of chronically infected patients, is linked with a high risk for hepatocellular carcinoma in later life (2, 3). To date, there is neither an effective immune globulin for prophylaxis nor a vaccine for the prevention of hepatitis C. The development of a safe and effective HCV vaccine remains a top priority for the global control of HCV infections.

The HCV envelope glycoprotein E2 has long been considered an important immunogenic target in efforts to develop an HCV vaccine candidate. This consideration is largely based on the role of the E2 protein in facilitating the entry of HCV into hepatocytes via interaction with the host entry factors (4–10). Recently, the crystal structure of the E2 core, in complex with a neutralizing antibody, was solved (11). The E2 core study described the interface crucial for host entry factor CD81-mediated entry, thus providing a site of vulnerability that can be exploited in immunogen design. The crystal structure also revealed that nearly 62% of the E2 core amino acid residues are either disordered or in loop structures, the overall effect of which indicates a striking flexibility in the E2 protein structures. Whether the intrinsic structural heterogeneity of the E2 protein is linked to the viral entry process or not is currently unknown.

Epitope II resides on the E2 protein between residues 427 and 446, a location that places it in the vicinity of the described E2–CD81 interface in the flexible area of the E2 protein (11–13). Paradoxically, different antibodies are able to bind to a similar set of residues on epitope II; however, their interactions with these residues can lead to either HCV neutralization or nonneutralization, as defined in an in vitro HCV cell culture system (12, 13). In addition, some epitope II-specific nonneutralizing antibodies were shown to interfere with the neutralization by antibodies at epitope I, another epitope on the E2 protein between residues 412 and 426 (12). Furthermore, depletion of these epitope II-specific antibodies revealed a broader cross-genotype neutralization by the epitope I-specific antibodies (14). Previously, we determined the crystal structure of epitope II in complex with an HCV-neutralizing antibody mAb#8, where mAb#8 interacts with epitope II through a bifurcated mode of action at two primary anchor sites within epitope II. Specifically, the antibody operates by means of hydrophobic interactions with residues Trp^{437} and Leu^{438} in the C-terminal α-helix and hydrophilic interactions with residues Glu^{431}/Asn^{434} in the N-terminal loop (15).

Here we report the crystal structure of epitope II in complex with mAb#12, an epitope II-specific antibody that lacks measurable activity of HCV neutralization in vitro (13). Furthermore, we compared the crystal structure of the mAb#12–epitope II complex with the known structures of other antibody–epitope II complexes. Our studies provide structural insights relevant to the site specificity of these functionally distinct epitope II-binding antibodies. We conclude that the particular spatial arrangements of the secondary structural elements in epitope II can determine how a specific antibody binds it and ultimately directs the outcomes of either antibody-mediated neutralization or nonneutralization.

Results

Overview of the Complex Structure. To obtain high-X-ray-diffraction-quality crystals suitable for structure determination, the Fab

Significance

X-ray crystallographic analysis revealed that one of the critical antibody-binding sites on the hepatitis C virus exists in different shapes. The structural transition among these shapes is governed by a highly conserved glycine residue that serves as a flexible joint connecting the two essential parts of the binding site; that is, the C-terminal α-helix and the N-terminal loop. It is the particular spatial arrangement of these parts that determines the specificity of antibody recognition and, consequently, the outcome of either neutralization or nonneutralization of the virus. These structural insights may be beneficial for the immune prophylaxis and treatment of HCV infections.

Author contributions: L.D. and P.Z. designed research; L.D., L.M., M.L.V., L.Z., H.Y., Z.Z., E.S., and P.Z. performed research; L.D. and P.Z. contributed new reagents/analytic tools; L.D., L.M., M.L.V., L.Z., H.Y., Z.Z., E.S., S.F., H.A., and P.Z. analyzed data; and L.D., M.L.V., L.Z., S.F., H.A., and P.Z. wrote the paper.

The authors declare no conflict of interest.

Freely available online through the PNAS open access option.

Data deposition: The atomic coordinates and structure factors have been deposited in the Protein Data Bank, www.pdb.org (PDB ID code 4Q0X).

[1]To whom correspondence may be addressed. Email: pei.zhang@fda.hhs.gov or halter@dtm.cc.nih.gov.

fragment of mAb#12, an antibody that binds to epitope II but is unable to neutralize the virus, was cocrystallized with synthetic peptides of different lengths, ranging from 13 to 35 mers, which encompass residues 412–446 of the E2 protein of the HCV H77 strain (13). Of the 6 peptides we have tested, only the 26-mer peptide (^{421}HINSTALNCNESLNTGWLAGLFYQHK^{446}) consisting of the entire epitope II and a portion of epitope I (12, 13) yielded sufficiently high-quality crystals for structure determination.

The structure of the mAb#12–epitope II complex was refined to 2.90-Å resolution (Table 1). A difference electron density map was calculated to reveal the peptide structure. The model building of the peptide was based exclusively on the visible-difference electron density map rather than the existing epitope II model from the structure of mAb#8–epitope II. Nine residues in the 26-mer peptide, from Asn^{434} to Phe^{442}, could be built successfully into a difference electron density map (Fig. 1*A*). The rest of the residues, including His^{421}–Leu^{433} of the N terminus and Tyr^{443}–Lys^{446} of the C terminus of the 26-mer peptide, were disordered.

Our previous study showed that the binding of mAb#12 to epitope II is relatively weaker than that of neutralizing antibody mAb#8 (13), which may be understood by analyzing these complex structures. Among the 13 residues of epitope II that participated in the interaction with mAb#8 (15), only nine were involved in binding to mAb#12, resulting in a smaller buried solvent-accessible surface area in the mAb#12–epitope II complex (1,112 Å^2 in mAb#12–epitope II vs. 1,478 Å^2 in mAb#8–epitope II). Contact residues in the mAb#12–epitope II complex were identified by measuring the distances between atoms, using the program CONTACT in CCP4 (16). Hydrogen bonds were calculated using a cutoff distance of 3.4 Å. The cutoff distance for van der Waals contacts was 4.0 Å. On the basis of these criteria, mAb#12 was found to make 90 contacts with epitope II, of which six are hydrogen bonds and 84 are van der Waals contacts. In contrast, mAb#8 makes substantially more contacts with epitope II: among its 134 contacts, 17 are hydrogen bonds and 117 are van der Waals contacts. The relative paucity of contacts in the mAb#12–epitope II interface contributes to its poor shape complementarity, according to the calculated shape correlation statistics of 0.67 (shape correlation = 1.0 for perfect fits) (17), compared with 0.72 for the interface between mAb#8 and epitope II. These differences may account for the weaker interaction of epitope II with mAb#12 compared with that with mAb#8.

Table 1. X-ray crystallographic statistics

Statistic	mAb#12–Epitope II
Data processing statistics	
Resolution limit, Å*	2.90 (3.12–2.95)
Space group	$P4_322$
Cell dimensions, Å, degrees	a = 49.99 c = 390.59
Unique reflections*	11,042 (1,502)
Completeness, %*	99.0 (99.9)
R_{merge}, %*	10.9 (27.2)
I/σ_I *	25.4 (5.9)
Refinement statistics	
R_{work}, %	22.1
R_{free}, %†	28.4
rmsds from ideality	
Bond lengths, Å	0.008
Bond angles, degrees	1.222
Ramachandran plot statistics	
Favored region, %	96.3
Allowed region, %	3.7

*Values in the parentheses are statistics of the highest resolution shell. †R_{free} is calculated for a randomly selected 5.0% of reflections not included in the refinement.

Epitope II Recognition by Nonneutralizing and Neutralizing Antibodies. As previously observed in the mAb#8–epitope II structure (15), the secondary structure of epitope II in mAb#12–epitope II is likewise composed of two major components: an N-terminal loop (residues 434–436) and a C-terminal 1.5-turn α-helix (residues 437–442) (Fig. 1 *B* and *C*). To understand the structural characteristics for epitope II recognition by nonneutralizing and neutralizing antibodies, we compared the interactions of epitope II with mAb#12 versus those with mAb#8. As in the case of mAb#8, the complementarity determining region (CDR) H3 loop of mAb#12 was positioned directly over the two key contact residues, Trp^{437} and Leu^{438} (Fig. 2 *A* and *B*), where amino acid substitutions could diminish the binding of epitope II by either mAb#8 or mAb#12, regardless of their capacity to neutralize the virus (13). Residue Trp^{437} is stabilized further by a hydrogen bond that forms between its side-chain N$^{\varepsilon 1}$ and an acidic residue: Asp^{99} in mAb#12 or Glu^{39} in mAb#8 (Fig. 2 *A* and *B*).

Despite certain resemblances, mAb#12 interacts with epitope II in markedly different ways from mAb#8. The number of residues of epitope II required for mAb#12 binding (i.e., Asn^{434}–Phe^{442}) is four residues fewer than that bound by mAb#8 (Asn^{430}–Phe^{442}). As a result, one of the anchors (Glu^{431}) that was identified in the mAb#8–epitope II structure cannot be established in the mAb#12–epitope II structure (Figs. 1 and 2) (15). In addition, the N-terminal loop of epitope II is loosely held by CDR1 and CDR2 of the heavy chain of mAb#12. In contrast, this loop is extensively involved in the hydrogen bond network with CDR2 and CDR3 of the heavy chain in mAb#8–epitope II (Fig. 2 *A* and *C*). Moreover, the hydrophobic patch of the C-terminal helix in mAb#12–epitope II is packed against CDR3 of the heavy chain and CDR2 and CDR3 of the light chain (Fig. 2*A*), whereas the helix is enwrapped by mAb#8 through all three heavy-chain CDR loops, as well as CDR1 and CDR3 of the light chain (Fig. 2*B*).

Superimposing the C-terminal helix of epitope II in the mAb#12–epitope II structure onto that in the mAb#8–epitope II structure revealed nearly identical conformations, including the residue side-chains of the helices, whereas the N-terminal loops of epitope II in the two structures adopted strikingly different conformations (Fig. 1 *B* and *C*). If one attempts to fit an epitope II that is based on the mAb#12–epitope II conformation into the binding groove of mAb#8 (or vice versa), it will not be possible because of the steric clash between the N-terminal loop and the antibody. This finding suggests that epitope II on the E2 protein of the virus can alternate between at least two discrete conformations: one that can be recognized by mAb#8 and another that can be recognized by mAb#12.

Comparisons of Epitope II from Different Crystal Structures. Two structures of the E2 core are currently available (11, 18); however, only the structure of the E2 core (residues 412–645), in complex with a neutralizing antibody, AR3C (11), includes epitope II (Fig. 3*A*). We compared the AR3C–E2 core with our antibody–epitope II complex structures (Fig. 3 *B* and *C*). The α-helix of epitope II is well-preserved across the three crystal structures, where the helical parts were superimposed. The side-chains of Trp^{437} and Leu^{438}, in particular, adopt almost identical conformations. However, the N-terminal loop of epitope II in AR3C–E2 core is positioned differently from that observed in mAb#12–epitope II and mAb#8–epitope II complexes. In each of the three complexes, the spatial arrangement of the N-terminal loop relative to the α-helical element was distinct. In all 6 HCV genotypes, Gly^{436} is almost never mutated to other

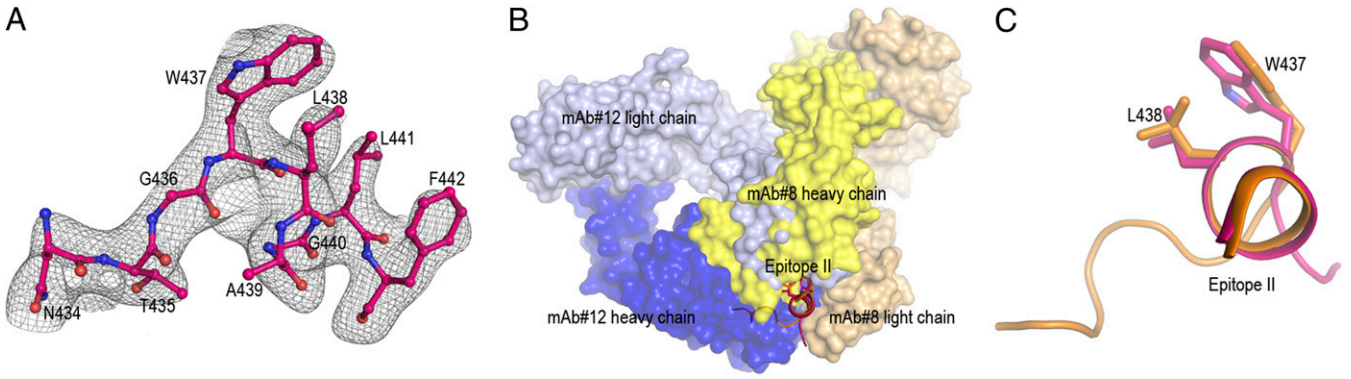

Fig. 1. Structure of epitope II in the mAb#12–epitope II complex and comparison with the mAb#8–epitope II complex. (*A*) The $2F_o$-F_c electron density map (contoured at 1σ) at 2.90-Å resolution with the ball-and-stick representation of epitope II from mAb#12–epitope II. (*B*) Superimposition of mAb#12–epitope II and mAb#8–epitope II complex shows the different orientations of the antibodies as they approach epitope II. Epitope II from mAb#12–epitope II is colored in magenta. Epitope II from mAb#8–epitope II is colored in orange. (*C*) A close-up view of the superimposition of epitope II in mAb#12–epitope II and mAb#8–epitope II.

residues, as seen by examining the 1,958 E2 protein sequences deposited in the National Institute of Allergy and Infectious Diseases Virus Pathogen Database and Analysis Resource (ViPR; www.viprbrc.org) (Table 2), and serves as a pivot point connecting the C-terminal α-helix and the N-terminal loop. The intrinsic flexibility of Gly^{436} with its remarkable conservation makes it an essential structural element in determining the general geometry of epitope II.

To establish quantitative and comparable measurements for the geometrical positions of the C-terminal α-helix relative to the N-terminal loop of epitope II, we calculated the angles formed between two straight lines that were drawn to represent the C-terminal α-helix and the N-terminal loop of epitope II. Of the three available structural models, mAb#12–epitope II was chosen as the base (Fig. 3*C*). One line was drawn from the C_α atom of Trp^{437} (the first residue of the helix) to the C_α atom of Phe^{442} (the last residue of the helix) of the epitope II, whereas the other was drawn from the C_α atom of Asn^{434} (the first residue of the N-terminal loop of the epitope II peptide in mAb#12–epitope II) to the C_α atom of Trp^{437}. The angles measured between the helix and the loop of epitope II, in mAb#12–epitope II, mAb#8–epitope II, and AR3C–E2 core were 114°, 75° and 142°, respectively (Fig. 3*C*). The observed angle deviations signify a dynamic conformational transition that can occur within epitope II.

We noticed that the epitope II residues Trp^{437} and Leu^{438}, which are crucial for binding by both nonneutralizing and neutralizing antibodies (mAb#12 and mAb#8), are partially buried under loop 8 of E2, which connects β-strands g and f in the AR3C–E2 core structure (Fig. 3*C*). As a result, epitope II in the AR3C–E2 core complex appears to be inaccessible to binding by either mAb#12 or mAb#8. A significant conformational change has to take place to fully expose both Trp^{437} and Leu^{438} to allow E2 recognition by mAb#12 or mAb#8. These observations led us to propose that the E2 protein may exist in two different states in terms of the presentation of epitope II: a closed state, as illustrated by the AR3C–E2 core, where residues Trp^{437} and Leu^{438} of epitope II are partially hidden, and an open state, where residues Trp^{437} and Leu^{438} are solvent accessible, as revealed by the structures of mAb#12–epitope II and mAb#8–epitope II.

In addition, we compared the AR3C–E2 core with the crystal structures of two other human anti-HCV neutralizing antibodies, HC84-27 and HC84-1 (19), in complex with epitope II (Fig. 3*D*). Residues Gly^{436}–Lys^{446} of epitope II were included in the structural models of HC84-27–epitope II and HC84-1–epitope II. As shown in Fig. 3*D*, the helical parts of epitope II in the complex structures are almost identical. The positioning of the antibodies indicates that HC84-27 and HC84-1 clearly recognize epitope II in the closed state of E2 protein, similar to the position shown in the AR3C–E2 core. However, the positions of the loops consisting of residues Tyr^{443}–Lys^{446} in HC84-27–epitope II and HC84-1–epitope II deviate significantly from the position of this loop in AR3C–E2 core, suggesting that local conformational

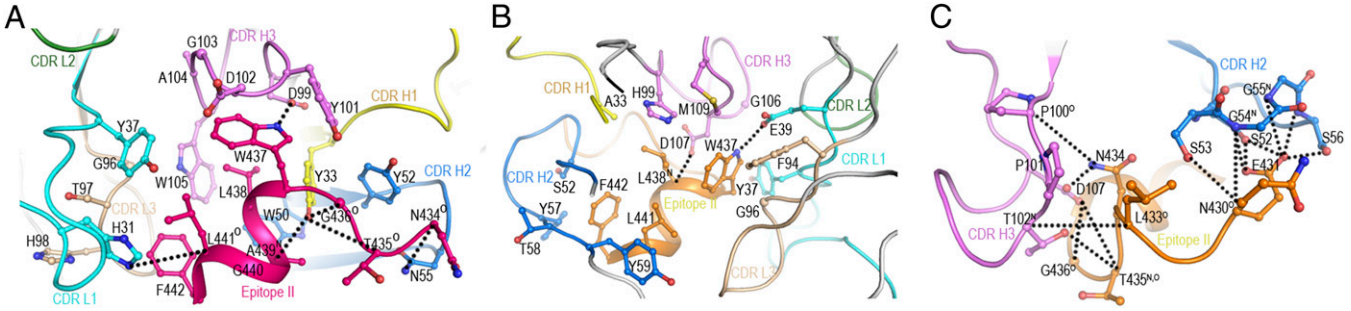

Fig. 2. Comparison of the different epitope II–antibody interfaces. The CDR loops are color-coded as follows: CDR H1 in yellow, CDR H2 in blue, CDR H3 in violet, CDR L1 in cyan, CDR L2 in green, and CDR L3 in wheat. Epitope II from mAb#12–epitope II is in magenta. Epitope II from mAb#8–epitope II is in orange. The side chains of interacting residues are drawn as ball-and-stick representations. Hydrogen bonds are represented by black dotted lines. (*A*) MAb#12–epitope II interface; (*B*) MAb#8–epitope II interface showing the interactions between mAb#8 and the C-terminal helix of epitope II; and (*C*) MAb#8–epitope II interface showing the interactions between mAb#8 and the N-terminal loop of epitope II.

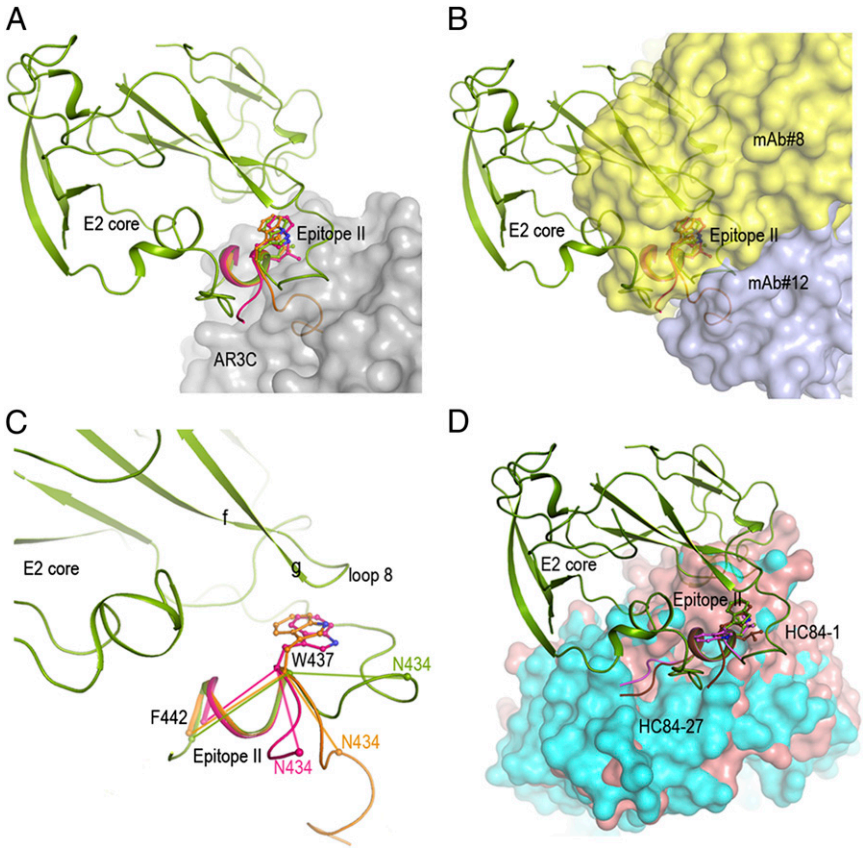

Fig. 3. Comparison of epitope II from different complex structures. The antibodies are shown as surface representations with AR3C in gray, mAb#12 in light blue, mAb#8 in yellow, HC84-27 in cyan, and HC84-1 in wheat. (*A*) Crystal structure of the AR3C–E2 core with its epitope II from the E2 core (green) overlaid with the corresponding epitope II from mAb#12–epitope II (magenta) and mAb#8–epitope II (orange). (*B*) The complex structures of mAb#12–epitope II and mAb#8–epitope II superimposed onto E2 core. (*C*) A close-up view of the superimposition of epitope II from the complex structures shows the angles formed between the helix and the loop of epitope II, in mAb#12–epitope II (magenta), mAb#8–epitope II (orange), and AR3C–E2 core (green). (*D*) Superimposition of epitope II from HC84-27–epitope II (violet) and HC84-1–epitope II (dark brown) onto E2 core.

changes are needed when epitope II is presented in the closed state of E2 to AR3C, HC84-27, and HC84-1.

Discussion

The critical role played by the E2 protein in the interactions with host receptors for HCV, particularly the key entry factor CD81, makes the E2 protein one of the most important targets for HCV vaccine design. A recent AR3C–E2 core study showed that CD81 binds to the same surface on the E2 core as the neutralizing antibody, AR3C, and thus defined the structural interface crucial for the E2–CD81 interaction (11). Although the structural determination of the E2 core singled out a promising site for immunogen design, it also confirmed a high degree of flexibility in E2. The E2 structure is inherently heterogeneous and includes several hypervariable regions and multiple *N*-linked glycans that are expected to affect, indirectly or directly, the optimal presentation of the immunogenic sites of interest. For vaccine development, it is thus essential to understand how the flexibility of E2 structures is controlled during the virus life cycle, especially during the viral entry process.

Our X-ray crystallographic analysis of epitope II in complex with mAb#12, an antibody that binds specifically to epitope II but is unable to neutralize the virus in vitro, showed an absence of the bifurcated mode of interaction with epitope II that was observed previously in the complex structure of neutralizing antibody mAb#8–epitope II (15). The binding of mAb#12 appears to be directed toward the C-terminal α-helix of epitope II with a reduced total number of contacts. Furthermore, the spatial arrangement of the essential components of epitope II, that is, the C-terminal α-helix and the N-terminal loop, which are bound by the nonneutralizing antibody mAb#12, departs significantly from that observed in the corresponding complex with neutralizing antibody. Therefore, within the open state of E2 when epitope II is exposed, at least two conformations are possible for these functionally distinct antibodies. It also should be mentioned that the structural basis for the role of interference associated with mAb#12 at epitope I, as shown in our previous biochemical studies (12, 13), could not be clearly addressed, although the peptide we used in the present study contains a part

Table 2. Sequence conservation of amino acid residues 434–442 (n = 1,958)

Position	Residue/number of strains in which it occurred								
434	**N**/1041	Q/348	D/235	H/162	E/64	R/11	S/32	T/9	X/7
435	**T**/1916	A34	S/5	X/2	P/1				
436	**G**/1957	E/1							
437	F/1219	**W**/730	L/3	C/3	X*/2	S/1			
438	I/835	**L**/831	V/248	F/25	X*/4	P/1	A/1		
439	**A**/1895	V/30	T/20	S/9	X*/2	K/1	H/1		
440	**G**/1249	A/569	S/132	X*/3	R/2	E/1	T/1	P/1	
441	**L**/1950	P/3	X*/2	C/1	S/1	V/1			
442	**F**/1697	L/136	I/109	M/7	V/5	X/3	S/1		

X*, residue not defined; bold, residues presented in this study.

of epitope I. In view of the AR3C–E2 core and our mAb#12–epitope II structures, epitope I is disordered. Further investigations are necessary to establish the structural relationship of these two epitopes for interpreting the phenomenon of interference.

Our results highlight that epitope II can be presented in different conformations on the E2 protein that determines the specificity of antibody recognition. Depending on the probability that HCV will present a particular form of epitope II on its surface, the host immune system may be skewed toward producing neutralizing or nonneutralizing antibodies against a specific conformation. This proposal may be related to the developmental pathways by which antibodies are generated in patients, wherein certain molecular characteristics are acquired during the affinity maturation of these antibodies. Clinically, it remains a paradox that broadly neutralizing antibodies directed to the E2 protein are rarely detected at the early stages of HCV infection. These neutralizing antibodies, if detectable at all, are essentially ineffective in vivo, despite neutralizing activity that can be demonstrated in vitro (20). It appears likely that such antibodies are overwhelmed by the substantial amounts of nonneutralizing antibodies already in circulation (14, 21). If epitope II is indeed undergoing structural transitions in vivo, this structural heterogeneity may become an important factor in determining how the neutralizing antibodies and nonneutralizing antibodies are elicited during the natural course of HCV infection.

The dynamic transition among these conformations could be expected to occur at epitope II on the E2 protein. This structural transition is made possible by the presence of Gly^{436}, which connects the C-terminal helix and the N-terminal loop of epitope II similar to a ball joint. The flexibility conferred by this highly conserved glycine residue meets the requirements for permitting the spatial and temporal relationships of the C-terminal α-helix and the N-terminal loop. This finding is consistent with the generally accepted role of glycine in providing the freedom necessary for the regulation of both folding and function of a protein (22–28). In addition, it has been found experimentally that Gly^{436} has a functional role in the entry process of the virus (6). More specifically, HCV entry was severely diminished by using E1–E2 pseudoparticles that contained a $G^{436}A$ or $G^{436}S$ substitution, which led to a corresponding loss of binding to the CD81 large extracellular loop (6). Intriguingly, the replacement of Gly^{436} by a proline residue on the E2 protein, which converted the flexible conformation of epitope II into a rigid structure, resulted in a significant loss of viral entry, even though the substitution did not diminish the ability of E2 to bind to CD81 (6). It therefore appears that the removal of the intrinsic flexibility conferred by Gly^{436} is, in itself, sufficient to affect virus entry into the liver cell.

Antibody-mediated neutralization of HCV can thus be viewed as the outcome from blocking access to the structurally defined E2–CD81 interface not only during the closed state of E2, when epitope II is hidden, but also during the open state of E2, when epitope II is fully exposed, from locking epitope II in a particular conformation that precludes virus entry into the liver cell. Conversely, if this transition process is taken advantage of by the virus, the virus may present an epitope II conformation that is capable of avoiding neutralization, thus allowing it to persist in patients. Although our study focused on the association between the specific tertiary structures of epitope II on the E2 and antibody-mediated neutralization and nonneutralization, it should not be interpreted as the sole mechanism for neutralization or nonneutralization occurring at epitope II. The potential role of the binding affinity of an antibody, for instance, in regulating its corresponding diverse bioactivities should not be ignored. Further examination of the binding kinetics and physicochemical properties of epitope II-specific antibodies should provide us with more comprehensive knowledge on this complicated biological process. Nonetheless, our structural insights into the key determinants of antibody-mediated neutralization and nonneutralization may contribute to, but are not limited to, the immune prophylaxis of HCV infection and the development of an effective HCV vaccine.

Materials and Methods

Protein Preparation and Peptide Synthesis. Ascites containing mAb#12 IgG were produced by Harlan Bioproducts for Science (Indianapolis, IN), as previously described (13). A HiTrap Protein G column (GE Healthcare Life Sciences, Piscataway, NJ) was used to extract the IgG from the ascites solution. The Fab fragment of mAb#12 was prepared with the Fab preparation kit from Thermo Scientific (Rockford, IL) by following the manufacturer's instructions. The Fab fragment was then further purified to homogeneity by a Mono S ion-exchange column (GE Healthcare Life Sciences). All peptides were chemically synthesized by the Core Laboratory of the Center for Biologics Evaluation and Research (CBER) at the US Food and Drug Administration (FDA), with an Applied Biosystems (Foster City, CA) model 433A peptide synthesizer. The mAb#12–epitope II complex was made by mixing the 26-mer peptide (^{421}HINSTALNCNESLNTGWLAGLFYQHK^{446}) with mAb#12 Fab (molar ratio of 4:1).

Crystallization and Data Collection. Crystallization screenings were carried out robotically with a Mosquito liquid dispenser (TTP LabTech, Cambridge, MA) by using the hanging-drop vapor diffusion method in a 96-well format and commercially available high-throughput screening kits (Hampton Research, Aliso Viejo, CA; Emerald Biosystems, Bainbridge Island, WA). Subsequent optimizations were done manually by mixing 1 μL protein and 1 μL precipitant solution. Crystals of the mAb#12–epitope II complex were grown in 0.1 M imidazole buffer (pH 7.0), and 14% (wt/vol) polyethylene glycol monomethyl ether 550 at 21 °C. Twenty percent glycerol was used as a cryoprotectant. X-ray diffraction data were collected at beamline ×29 of the Brookhaven National Synchrotron Light Source with an ADSC Quantum-315 CCD detector (Brookhaven National Laboratory, Upton, NY). All data were indexed, integrated, and scaled with the program HKL2000 (29). Data collection statistics are in Table 1.

Structure Determination and Refinement. Orientation and position parameters for the structure of the mAb#12–epitope II complex were obtained by molecular replacement with the program Phaser (30) in the CCP4 program suite (16). The search model is the anticholera toxin antibody (PDB ID code 1ZEA). The CDR loops were deleted in the initial refinement with RefMac 5.0 (31) and built into positions where an unambiguous electron density was shown with the program COOT (32). The difference electron-density map clearly showed the peptide at the mAb#12 antigen binding site. The peptide was then built into electron density. Final refinement statistics are in Table 1. Contact residues in the mAb#12–epitope II complex were identified with the program CONTACT in CCP4 and were defined as residues containing an atom ≤ 4.0 Å from a residue of the binding partner (16). Buried surface areas were calculated by the program AREAIMOL in CCP4 with a 1.4-Å probe radius (16). PyMOL (www.pymol.org) was used to prepare the structural figures.

ACKNOWLEDGMENTS. We thank Dr. John Finlayson for his comments on the manuscript, Dr. Tsan Xiao and Dr. Tengchuan Jin (National Institute of Allergy and Infectious Diseases) for providing the instrument for crystallization screening, Dr. Hongying Duan (CBER/FDA) for providing the monoclonal antibody reagents, and the FDA CBER Core Laboratory for assisting in protein sequence analysis. We also thank Howard Robinson (Brookhaven National Synchrotron Light Source) for X-ray data collection. Beamline X29 is supported by the US Department of Energy Offices of Biological and Environmental Research and Basic Energy Sciences and by the National Center for Research Resources of the National Institutes of Health. This study was funded by a Modernizing Science grant from CBER, FDA. L.M. and Z.Z. were supported by the Research Participation Program at CBER administered by the Oak Ridge Institute for Science and Education through an interagency agreement between the US Department of Energy and the FDA.

1. Centers for Disease Control and Prevention (2012) *CDC Health Information for International Travel* (Oxford Univ Press, New York).
2. Alter HJ, Seeff LB (2000) Recovery, persistence, and sequelae in hepatitis C virus infection: A perspective on long-term outcome. *Semin Liver Dis* 20(1):17–35.
3. Ghany MG, Strader DB, Thomas DL, Seeff LB; American Association for the Study of Liver Diseases (2009) Diagnosis, management, and treatment of hepatitis C: An update. *Hepatology* 49(4):1335–1374.
4. Pileri P, et al. (1998) Binding of hepatitis C virus to CD81. *Science* 282(5390):938–941.

5. Flint M, et al. (1999) Characterization of hepatitis C virus E2 glycoprotein interaction with a putative cellular receptor, CD81. *J Virol* 73(8):6235–6244.
6. Drummer HE, Boo I, Maerz AL, Poumbourios P (2006) A conserved Gly436-Trp-Leu-Ala-Gly-Leu-Phe-Tyr motif in hepatitis C virus glycoprotein E2 is a determinant of CD81 binding and viral entry. *J Virol* 80(16):7844–7853.
7. Ray R, et al. (2010) Characterization of antibodies induced by vaccination with hepatitis C virus envelope glycoproteins. *J Infect Dis* 202(6):862–866.
8. Law M, et al. (2008) Broadly neutralizing antibodies protect against hepatitis C virus quasispecies challenge. *Nat Med* 14(1):25–27.
9. Dorner M, et al. (2013) Completion of the entire hepatitis C virus life cycle in genetically humanized mice. *Nature* 501(7466):237–241.
10. Zhao Z, et al. (2014) A neutralization epitope in the hepatitis C virus E2 glycoprotein interacts with host entry factor CD81. *PLoS ONE* 9(1):e84346.
11. Kong L, et al. (2013) Hepatitis C virus E2 envelope glycoprotein core structure. *Science* 342(6162):1090–1094.
12. Zhang P, et al. (2007) Hepatitis C virus epitope-specific neutralizing antibodies in Igs prepared from human plasma. *Proc Natl Acad Sci USA* 104(20):8449–8454.
13. Duan H, et al. (2012) Amino acid residue-specific neutralization and nonneutralization of hepatitis C virus by monoclonal antibodies to the E2 protein. *J Virol* 86(23): 12686–12694.
14. Zhang P, et al. (2009) Depletion of interfering antibodies in chronic hepatitis C patients and vaccinated chimpanzees reveals broad cross-genotype neutralizing activity. *Proc Natl Acad Sci USA* 106(18):7537–7541.
15. Deng L, et al. (2013) Structural evidence for a bifurcated mode of action in the antibody-mediated neutralization of hepatitis C virus. *Proc Natl Acad Sci USA* 110(18): 7418–7422.
16. Collaborative Computational Project, Number 4 (1994) The CCP4 suite: Programs for protein crystallography. *Acta Crystallogr D Biol Crystallogr* 50(Pt 5):760–763.
17. Lawrence MC, Colman PM (1993) Shape complementarity at protein/protein interfaces. *J Mol Biol* 234(4):946–950.
18. Khan AG, et al. (2014) Structure of the core ectodomain of the hepatitis C virus envelope glycoprotein 2. *Nature* 509(7500):381–384.
19. Krey T, et al. (2013) Structural basis of HCV neutralization by human monoclonal antibodies resistant to viral neutralization escape. *PLoS Pathog* 9(5):e1003364.
20. Logvinoff C, et al. (2004) Neutralizing antibody response during acute and chronic hepatitis C virus infection. *Proc Natl Acad Sci USA* 101(27):10149–10154.
21. Burioni R, et al. (2001) Nonneutralizing human antibody fragments against hepatitis C virus E2 glycoprotein modulate neutralization of binding activity of human recombinant Fabs. *Virology* 288(1):29–35.
22. Creighton TE (1994) *Proteins: Structures and Molecular Properties*. 2nd ed (WH Freeman, New York).
23. Yan BX, Sun YQ (1997) Glycine residues provide flexibility for enzyme active sites. *J Biol Chem* 272(6):3190–3194.
24. Stanfield R, et al. (1999) Dual conformations for the HIV-1 gp120 V3 loop in complexes with different neutralizing fabs. *Structure* 7(2):131–142.
25. Sharon M, et al. (2003) Alternative conformations of HIV-1 V3 loops mimic beta hairpins in chemokines, suggesting a mechanism for coreceptor selectivity. *Structure* 11(2):225–236.
26. Rosen O, et al. (2005) Induced fit in HIV-neutralizing antibody complexes: Evidence for alternative conformations of the gp120 V3 loop and the molecular basis for broad neutralization. *Biochemistry* 44(19):7250–7258.
27. Scheib H, Sperisen P, Hartley O (2006) HIV-1 coreceptor selectivity: Structural analogy between HIV-1 V3 regions and chemokine beta-hairpins is not the explanation. *Structure* 14(4):645–647, discussion 649–651.
28. Zolla-Pazner S, Cardozo T (2010) Structure-function relationships of HIV-1 envelope sequence-variable regions refocus vaccine design. *Nat Rev Immunol* 10(7):527–535.
29. Otwinowski Z, Minor W (1997) Processing of X-ray diffraction data collected in oscillation mode. *Methods Enzymol* 276(Pt A):307–326.
30. Storoni LC, McCoy AJ, Read RJ (2004) Likelihood-enhanced fast rotation functions. *Acta Crystallogr D Biol Crystallogr* 60(Pt 3):432–438.
31. Murshudov GN, Vagin AA, Dodson EJ (1997) Refinement of macromolecular structures by the maximum-likelihood method. *Acta Crystallogr D Biol Crystallogr* 53(Pt 3): 240–255.
32. Emsley P, Lohkamp B, Scott WG, Cowtan K (2010) Features and development of Coot. *Acta Crystallogr D Biol Crystallogr* 66(Pt 4):486–501.